

Photoionisation Mass-spectrometric Study of Fragmentation of SiBr₄ and GeBr₄ in the Range 400–1220 Å

Jeremy C. Creasey, Ian R. Lambert and Richard P. Tuckett*

School of Chemistry, University of Birmingham, Edgbaston, Birmingham B15 2TT, UK

Keith Codling, Leszek J. Frasinski, Paul A. Hatherly and Marek Stankiewicz

J. J. Thompson Physical Laboratory, University of Reading, Whiteknights, Reading RG6 2AK, UK

The non-radiative decay channels of the valence electronic states of SiBr₄⁺ and GeBr₄⁺ have been studied in the range 1220–400 Å (10–31 eV) by photoionisation mass spectrometry. Ion-yield curves for the parent ions and for MBr₃⁺, MBr₂⁺, MBr⁺, M⁺ and Br⁺ (M = Si, Ge) have been obtained, as well as the relative photoionisation branching ratios. The appearance thresholds for SiBr₃⁺ and GeBr₃⁺ occur at 11.31 and 10.97 eV, respectively. They lie within the Franck–Condon region of the ground state of SiBr₄⁺ and GeBr₄⁺, and are at the thermodynamic thresholds for SiBr₃⁺ + Br and GeBr₃⁺ + Br. The smaller fragment ions have appearance thresholds which relate to energies of excited electronic states of SiBr₄⁺ and GeBr₄⁺, and not to the lower-lying thermodynamic energy of the fragment ion. The results are discussed with reference to our earlier work on radiative decay from excited states of SiBr₄⁺ and GeBr₄⁺ (*J. Chem. Soc., Faraday Trans.*, 1990, **86**, 2021). We have obtained a new value for the ionisation potential of SiBr₃ of 7.6 ± 0.4 eV, and we suggest that the previously accepted value for SiBr₂ (12 ± 1 eV) is ca. 3.5 eV too high.

We have recently reported^{1–6} the observation of electronic emission spectra of several Group 14 tetrahalide molecular ions MX₄⁺ (M = C, Si, Ge; X = F, Cl, Br). Dispersed fluorescence spectra have been observed at a low rotational temperature in a crossed molecular beam/electron beam apparatus, and at room temperature with He* metastable (19.8 eV) Penning ionisation. Undispersed spectra have been observed at room temperature using photons from a synchrotron as a tunable source of vacuum UV radiation, thereby establishing the energy thresholds for fluorescence. The chlorides and bromides of MX₄⁺ show very similar radiative decay properties. Emission is observed from the third excited state (\tilde{C}^2T_2) of SiCl₄⁺, GeCl₄⁺, SiBr₄⁺ and GeBr₄⁺ and all these states have long radiative lifetimes in the range 38–67 ns. The fourth and highest valence state (\tilde{D}^2A_1) of these ions does not fluoresce, nor do any states of CCl₄⁺ and CBr₄⁺. By contrast the three fluorides of MX₄⁺ show radiative decay from the \tilde{D}^2A_1 state, and only the \tilde{C}^2T_2 state of CF₄⁺ decays by photon emission to any measurable extent. The observation of emission from any of these excited states is surprising, because it means that these states are bound, despite the fact that they can lie several eV above a number of dissociation channels. In such circumstances non-radiative decay by fragmentation would be expected to be the dominant decay mechanism, especially in such large five-atom polyatomic molecules.

Complementary experiments are being performed at the synchrotron source to investigate the non-radiative processes occurring in these valence ionic states. We use a technique which combines the photoelectron–photoion coincidence (PEPICO) experiment with a continuously tunable photon source.^{7,8} Radiation from the synchrotron storage ring photoionises MX₄, and the ionic dissociation products are detected in delayed coincidence with photoelectrons by time-of-flight (TOF) mass spectrometry, allowing thresholds for fragmentation channels to be determined. From an analysis of the TOF peak shape it is possible to determine the kinetic energy imparted to the ionic fragment.⁸ These experiments have already been described for the Group 14 fluorides and chlorides,⁷ and this paper describes the results for SiBr₄ and GeBr₄. The low vapour pressure of CBr₄ at room temperature precluded its study. This is the first reported photoionisation mass spectrum of SiBr₄ and GeBr₄, and we have

established new values for the ionisation potentials (E_i) of SiBr₃ and SiBr₂. The former E_i (7.6 eV) is 4.8 eV lower than the previously accepted value in the literature.

Experimental

Synchrotron radiation from the SERC 2 GeV electron storage ring at Daresbury is dispersed by a 1 m Seya monochromator and introduced into a stainless-steel chamber *via* a 100 mm long, 2 mm i.d. glass capillary. Vacuum UV radiation in the range 1220–400 Å (10.2–31.0 eV) is used at a bandpass of 4 Å. Two gratings with 1200 lines mm⁻¹ mounted back-to-back on a single kinematic mount in the Seya are available to span this region; in this paper they will be referred to as the high-energy grating (840–400 Å) blazed at 600 Å, and the low-energy grating (1220–600 Å) blazed at 850 Å. The wavelength calibration of the monochromator is accurate to better than 1 Å,⁹ and over these wavelength ranges the second-order contribution from the two gratings is negligible. SiBr₄ and GeBr₄ vapour is introduced to the whole chamber through a fine precision needle valve (Edwards FCV10K). The chamber is pumped by a 330 dm³ s⁻¹ turbo molecular pump. The base pressure is ca. 5 × 10⁻⁷ Torr, during an experiment the gas pressure in the whole chamber is constant at (1–2) × 10⁻⁵ Torr. Two identical TOF drift tubes lie orthogonal to and equidistant from the direction of the vacuum UV photon beam. An extraction field of 78.5 V cm⁻¹ accelerates electrons into one tube, ions into the other, and the photoionisation products are detected by two pairs of microchannel plates. The grid configuration and potentials in the TOF tubes satisfy the space-focussing condition.¹⁰ Correlated electrons and ions from the same ionisation event are detected in delayed coincidence, producing a PEPICO spectrum. The TOF data are processed using CAMAC electronics, and the experiment is controlled by two interacting computers. An IBM-PC/AT with colour graphics sets the experimental parameters, displays the data in real time and stores it on disc. An LSI 11/23 scans the grating in the Seya monochromator, and stores the total ion and electron count rates (amongst other auxiliary measurements).

Synchrotron flux is monitored by a window coated with sodium salicylate and a photomultiplier tube. Flux normalisation is achieved by recording coincidences at a fixed

photon wavelength until the accumulated number of counts from the photomultiplier tube reaches a preset value. The excitation wavelength is then stepped on and the process repeated. Data accumulate as a three-dimensional histogram of photon wavelength *vs.* ion TOF *vs.* coincidences, the last variable being represented by colour on the IBM-PC. In this paper the data are displayed in the form of two-dimensional photoionisation yield curves. Other representations (including the original 3D histograms) are shown elsewhere.⁹ From the width of a TOF peak it is possible to estimate the energy released into translational kinetic energy of the fragments. Details are given elsewhere.⁸ We have not attempted to measure such releases in the fragments involving one or more bromine atoms because of the inherent broadening of a TOF peak due to the two bromine isotopes (⁷⁹Br = 50%, ⁸¹Br = 50%). One such measurement, however, was made on the Si⁺ fragment.

Ultrapure SiBr₄ and GeBr₄ were supplied by Alfa Products (Johnson Matthey). These compounds are liquids at room temperature with vapour pressures of *ca.* 5 and 1 Torr, respectively. They underwent several freeze-pump-thaw cycles prior to use, and the liquids were held at room temperature in a water Dewar. The low vapour pressure of the two bromides precluded us from introducing the sample to the chamber through a narrow stainless-steel needle orthogonal to the photon flux, as used in previous experiments on the Group 14 fluorides and chlorides⁷ and SF₆.⁸ Thus the pressure in the whole chamber is constant, and there is no reduction in the translational temperature of the parent MBr₄ from room temperature.

Valence Ionic States and Ionic Dissociation Channels of SiBr₄⁺ and GeBr₄⁺

The valence molecular orbitals (MOs) of MBr₄ are very similar to those of the corresponding tetrafluorides and tetrachlorides.^{4,5} Electron removal from the five highest occupied MOs of MBr₄ gives rise to the five valence states of MBr₄⁺: \tilde{X}^2T_1 , \tilde{A}^2T_2 , \tilde{B}^2E , \tilde{C}^2T_2 and \tilde{D}^2A_1 . He I photoelectron spectroscopy¹¹ shows that substantial spin-orbit splitting is observed in the triply degenerate t₁ and t₂ orbitals, and the ionisation potentials (*E_i*s) of these states are shown in Table 1. No vibrational structure is resolved in any photoelectron band, so vertical *E_i*s are quoted, due to the difficulty of estimating an adiabatic *E_i* from a continuous photoelectron band. The energies of the ionic dissociation channels open to these valence states of SiBr₄⁺ and GeBr₄⁺ are also given in Table 1. These values come from the best data available for the neutral heats of formation¹² and *E_i*s for the species MBr_{*n*}, where *n* = 1–3. However, in contrast to the tetrafluorides and tetrachlorides, some of these data have either not been measured directly or are not well established. The uncertainties involved in these calculations were discussed in our earlier paper on the radiative decay properties of SiBr₄⁺ and GeBr₄⁺.⁶ In particular we commented on the following points: (a) The best available thermodynamics place the lowest dissociation channel of SiBr₄⁺ to SiBr⁺ + Br₂ + Br at 3.1 ± 0.7 eV above the ground state of SiBr₄⁺. This suggests that the \tilde{X} , \tilde{A} and \tilde{B} states of SiBr₄⁺ are all bound with deep minima in their potential surfaces, and would contradict the apparent continuous nature of the SiBr₄⁺ \tilde{C} - \tilde{A} and \tilde{C} - \tilde{X} fluorescence bands.⁶ (b) The ordering of the dissociation channels of SiBr₄⁺ in Table 1 is different from the pattern observed in the Group 14 fluorides and chlorides.^{4,5} In each of these cases the MX₃⁺ + X channel has the lowest energy and the \tilde{X} , \tilde{A} and \tilde{B} states of MX₄⁺ dissociate into this channel. We suggested⁶ that there might a gross error in the energy of the SiBr₃⁺ + Br channel at 16.2 eV (which uses the value of the

Table 1 Energetics of dissociation channels of SiBr₄⁺ and GeBr₄⁺

neutral/parent ion	ionic dissociation channel	dissociation energy/eV	vertical ^a <i>E_i</i> /eV		
SiBr ₄ ⁺ \tilde{D}^2A_1	SiBr + Br ₂ + Br ⁺	19.2	17.31		
	SiBr + Br ₂ ⁺ + Br	17.9			
	SiBr ₂ ⁺ + Br + Br	17.8			
	SiBr ₂ + Br + Br ⁺	17.7			
	Si ⁺ + Br ₂ + Br ₂	16.3			
	SiBr ₃ ⁺ + Br	16.2			
	SiBr ⁺ + 3Br	16.0			
	SiBr ₂ ⁺ + Br ₂	15.8			
	SiBr ₃ + Br ⁺	15.5			
	SiBr ₂ + Br ₂ ⁺	14.4			
	SiBr ⁺ + Br ₂ + Br	14.0			
	SiBr ₄ ⁺ \tilde{C}^2T_2				13.92
		SiBr ₄ ⁺ \tilde{B}^2E			12.33
				SiBr ₄ ⁺ \tilde{A}^2T_2	
SiBr ₄ ⁺ \tilde{X}^2T_1					10.9
			SiBr ₄ ⁺ \tilde{X}^1A_1		0
GeBr ₄ ⁺ \tilde{D}^2A_1	GeBr + Br ₂ + Br ⁺	18.4		17.6	
	GeBr + Br ₂ ⁺ + Br	17.1			
	GeBr ₂ + Br + Br ⁺	16.3			
	GeBr ⁺ + 3Br	15.6			
	GeBr ₂ ⁺ + Br + Br	14.1			
	GeBr ₄ ⁺ \tilde{C}^2T_2				13.63
		GeBr ⁺ + Br ₂ + Br	13.6		
		GeBr ₂ + Br ₂ ⁺	13.0		
	GeBr ₄ ⁺ \tilde{B}^2E				11.89
		GeBr ₄ ⁺ \tilde{A}^2T_2			11.23
GeBr ₄ ⁺ \tilde{X}^2T_1	GeBr ₃ ⁺ + Br		11.0		
	GeBr ₄ ⁺ \tilde{X}^1A_1		0		

^a From ref. 11. For the ²E, ²T₂ and ²T₁ ionic states, energy of the lower spin-orbit state only is shown.

appearance potential of SiBr₃⁺ from an SiBr₃ precursor in an electron-impact mass spectrometer¹³), and that it would be interesting to compare with the appearance energy of SiBr₃⁺ from SiBr₄ in a photoionisation mass spectrometer. Similarly, uncertainty was expressed in the energy of the SiBr₂⁺ + Br₂ channel at 15.8 eV. (c) Heats of formation are known for GeBr₄, GeBr₂ and GeBr. The only datum available for GeBr₃ is an electron-impact appearance potential of GeBr₃⁺ from GeBr₄,¹⁴ which places the GeBr₃⁺ + Br channel very close in energy to the \tilde{X}^2T_1 ground state of GeBr₄⁺. However, by contrast with SiBr₄⁺, the ordering of the dissociation channels of GeBr₄⁺ is much as expected if a comparison with the Group 14 fluorides and chlorides is valid.

Results

Ion-yield Curves from Photot ionisation of SiBr₄⁺

Ionic fragmentation of SiBr₄ excited by vacuum UV radiation was studied between 550 and 1220 Å (22.5–10.2 eV), a wavelength region that encompasses the five valence electronic states of SiBr₄⁺ (Table 1). This range was covered in six scans, five using the low-energy grating (690–1220 Å) and one the high-energy grating (550–790 Å). The bandpass of the Seya monochromator was 4 Å throughout, and the wavelength increment was *ca.* 1 Å per step. In the TOF window used (4.16–12.34 μs) four peaks are observed centred at 10.77, 9.47, 7.92 and 5.98 μs. They correspond to SiBr₄⁺, SiBr₃⁺, SiBr₂⁺ and SiBr⁺, respectively, the SiBr₂⁺ peak being especially weak. Photofragmentation was also studied with the high-energy grating between 400 and 645 Å with a different

TOF window (1.92–10.10 μs), and now peaks at 5.17 and 3.05 μs are observed, corresponding to Br^+ and Si^+ , respectively.

The ion yield curve of SiBr_4^+ (Fig. 1) is obtained by taking a cut through the 3D histogram, and integrating over the TOF range corresponding to the SiBr_4^+ ion (10.66–10.91 μs). The threshold for production of the parent ion is $1167 \pm 4 \text{ \AA}$ ($10.62 \pm 0.04 \text{ eV}$), which compares excellently with the adiabatic E_i of $\text{SiBr}_4^+ \bar{X}^2T_1$ as measured by photoelectron spectroscopy.¹¹ Although adiabatic E_i s are not quoted in ref. 11 they have been estimated from the published spectrum. However, the photoionisation measurement reported here is a more accurate figure. (In this paper thresholds are measured as the photon wavelength at which the signal rises out of the background noise.) A second threshold is observed at $1085 \pm 6 \text{ \AA}$ ($11.38 \pm 0.06 \text{ eV}$) corresponding to the adiabatic E_i of the \bar{A}^2T_2 first excited state of SiBr_4^+ . Two more apparent thresholds are observed at $1012 \pm 5 \text{ \AA}$ ($12.25 \pm 0.06 \text{ eV}$) and $865 \pm 5 \text{ \AA}$ ($14.33 \pm 0.08 \text{ eV}$). The shape of the ion-yield curve represents the variation of the total photoionisation cross-section with photon energy. For energies which can access several electronic states of SiBr_4^+ , the total cross-section will have contributions from all these states weighted by their partial ionisation cross-sections, and the peaks at 790, 985 and 1060 \AA are probably due to shape resonances caused by an enhanced cross-section into one or more electronic state. Absolute values for the total or partial ionisation cross-sections have not been measured for SiBr_4^+ .

The ion-yield curve of SiBr_3^+ is shown in Fig. 2. A threshold is observed weakly at $1096 \pm 4 \text{ \AA}$ ($11.31 \pm 0.03 \text{ eV}$) followed by a large and sharp increase in SiBr_3^+ signal with threshold of $1083 \pm 3 \text{ \AA}$ ($11.44 \pm 0.03 \text{ eV}$). A further apparent new threshold is observed at $1012 \pm 5 \text{ \AA}$ ($12.25 \pm 0.06 \text{ eV}$). The first threshold lies in the high-energy part of the \bar{X}^2T_1 ground-state photoelectron band, the second threshold corresponds well with the adiabatic energy of the lower spin-orbit component of \bar{A}^2T_2 (see above), whilst the third threshold lies between the vertical E_i s of the nearly degenerate higher spin-orbit component of \bar{A}^2T_2 and \bar{B}^2E . For wavelengths below these thresholds it is noted that the broad peaks at *ca.* 790 and 985 \AA are also observed in the SiBr_4^+ ion-yield curve.

The ion-yield curves for SiBr_2^+ and SiBr^+ between 400 and 790 \AA are shown in Fig. 3 and 4. Both channels are weak and background (false) coincidences have been subtracted from the spectra. Thresholds are observed at $770 \pm 12 \text{ \AA}$ ($16.1 \pm 0.3 \text{ eV}$) in the SiBr_2^+ channel and $724 \pm 12 \text{ \AA}$ ($17.1 \pm 0.3 \text{ eV}$) in the SiBr^+ channel. By taking TOF spectra at photon wavelengths above and below these thresholds, we have confirmed that these are genuine values, and that the

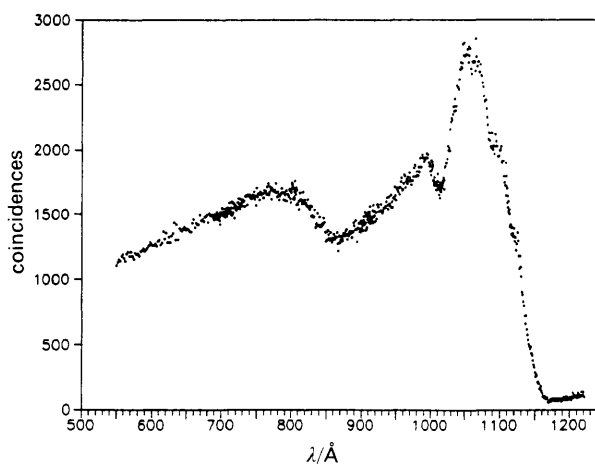


Fig. 1 Photoionisation yield of SiBr_4^+ from SiBr_4 in the range 550–1220 \AA

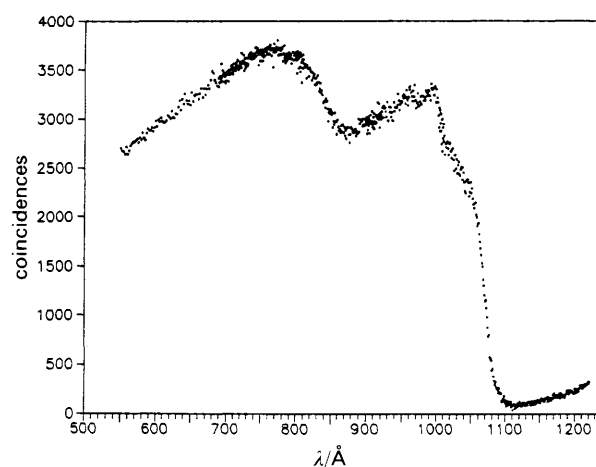


Fig. 2 Photoionisation yield of SiBr_3^+ from SiBr_4 in the range 550–1220 \AA

SiBr_2^+ ion is present at lower excitation energies than the SiBr^+ ion. Since both channels are weak care must be taken not to overinterpret these data. However, a comparison of Fig. 3 and 4 shows that the gross features of the SiBr_2^+ and SiBr^+ ion-yield curves are different. Thus whilst the SiBr_2^+ signal reaches a maximum around 650–700 \AA , SiBr^+ attains a maximum around 530 \AA . Therefore we believe that the

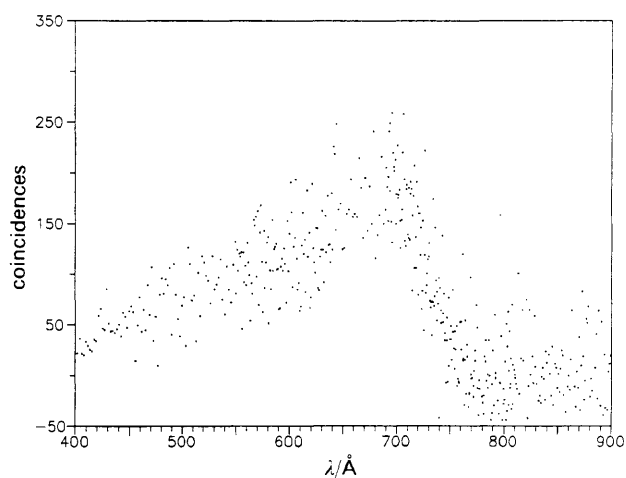


Fig. 3 Photoionisation yield of SiBr_2^+ from SiBr_4 in the range 400–900 \AA . False coincidences have been subtracted

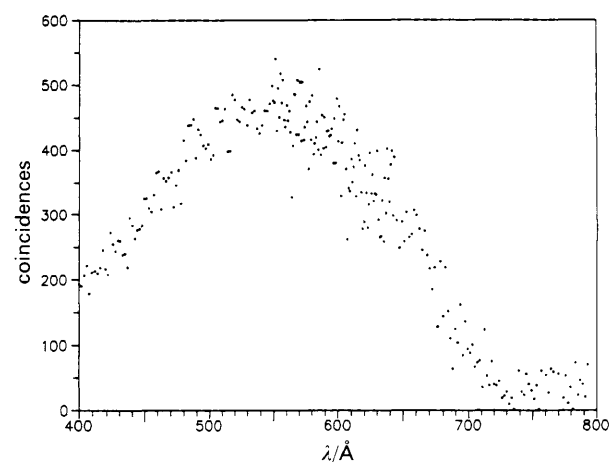


Fig. 4 Photoionisation yield of SiBr^+ from SiBr_4 in the range 400–790 \AA . False coincidences have been subtracted

SiBr_2^+ and SiBr^+ fragment ions result from dissociation of different initial states. The $\tilde{\text{D}}^2\text{A}_1$ state of SiBr_4^+ has an adiabatic E_i (16.85 ± 0.15 eV)¹¹ close to the appearance energy of SiBr^+ , and does not decay radiatively.⁶ The shape of the SiBr^+ ion yield is characteristic of a non-resonant photoionisation process, and therefore we believe the $\tilde{\text{D}}^2\text{A}_1$ state of SiBr_4^+ dissociates non-radiatively to this fragment ion. The origin of the very weak SiBr_2^+ signal is not well understood. It is very unlikely to be due to second-order radiation from the Seya monochromator since SiBr_2^+ is present over the wide wavelength range of 400–743 Å. Furthermore, a scan between 350 and 590 Å did not show any enhancement in SiBr_2^+ signal at half the observed threshold, *i.e.* at 385 Å. This channel is discussed further later.

The ion-yield curves for the Si^+ and Br^+ atomic ions are shown in Fig. 5 and 6. The thresholds are 530 ± 10 Å (23.4 ± 0.4 eV) and 496 ± 10 Å (25.0 ± 0.5 eV), respectively. Unfortunately a He II photoelectron spectrum of SiBr_4 is not available, and therefore these thresholds cannot be compared with the energies of higher-lying electronic states of the parent ion. Neither is it possible to compare the intensities of these atomic ions with the intensities of all the molecular ions, because the TOF window used in these experiments excludes the parent ion SiBr_4^+ . However the Si^+ and Br^+ channels acquire substantial intensity above threshold; for example, at 400 Å the relative intensities of $\text{Si}^+ : \text{Br}^+ : \text{SiBr}_3^+$ are 0.27 : 0.66 : 1.00. For $\lambda > 550$ Å it is possible to calculate the mass-spectrometric branching ratios for photoionisation, and these are shown in Fig. 7 for photon energies down to 11

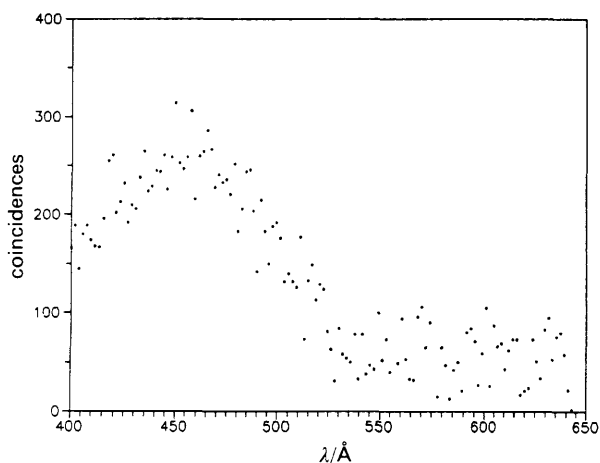


Fig. 5 Photoionisation yield of Si^+ from SiBr_4 in the range 400–645 Å

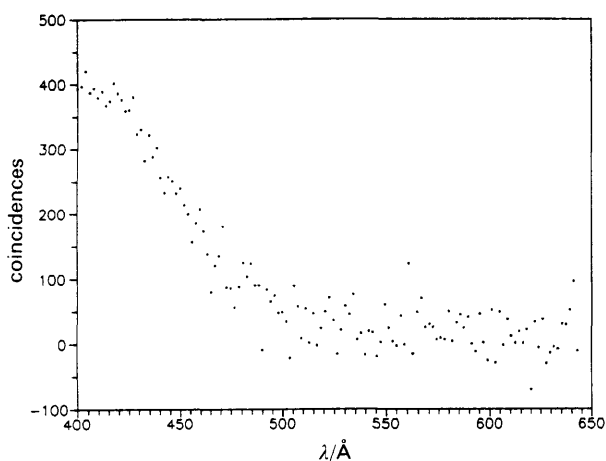


Fig. 6 Photoionisation yield of Br^+ from SiBr_4 in the range 400–645 Å

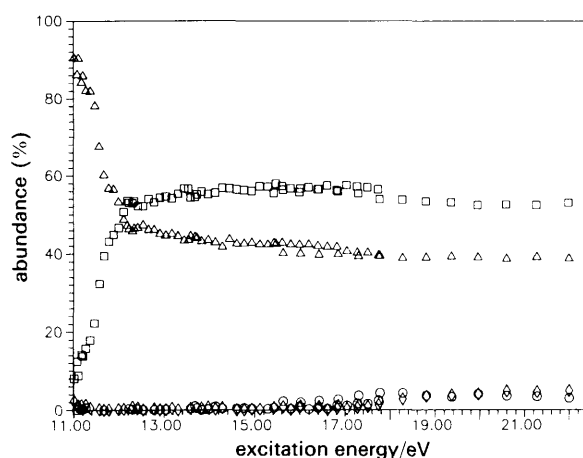


Fig. 7 Normalised photoionisation branching ratios for fragmentation of SiBr_4 between 11 and 22 eV. \diamond , SiBr^+ ; \circ , SiBr_2^+ ; \square , SiBr_3^+ ; \triangle , SiBr_4^+

eV. These ratios represent the relative abundance of ions (parent and fragments) at a defined photon energy. Note that this is different from a normalised 'breakdown diagram' which depicts the relative abundance of ions at a defined internal energy of the parent ion.¹⁵

Ion-Yield Curves from Photoionisation of GeBr_4

Ionic fragmentation of GeBr_4 was studied between 450 and 1200 Å. This range was covered in four scans, two using the low-energy grating (750–1200 Å) and two the high-energy grating (450–840 Å). The bandpass of the Seya monochromator was 4 Å, and the wavelength increment was *ca.* 2 Å per step. In the TOF window used (4.16–12.34 μs) five peaks are observed centred at 11.44, 10.21, 7.15, 5.14 and 4.93 μs, corresponding to GeBr_4^+ , GeBr_3^+ , GeBr^+ , Br^+ and Ge^+ , respectively. A very weak peak at 9.47 μs with an apparent threshold at 810 ± 25 Å is due to GeBr_2^+ . The signal is strongest in the 700–800 Å region, but is undetectable below 650 Å (unlike the SiBr_2^+ channel), and we believe this signal is due to second-order radiation.

The ion-yield curve for GeBr_4^+ is shown in Fig. 8. A threshold is observed at 1167 ± 4 Å (10.62 ± 0.04 eV), and we believe this is the most reliable measurement of the adiabatic E_i of $\text{GeBr}_4^+ \tilde{\text{X}}^2\text{T}_1$. Our estimate of this value from the published photoelectron spectrum¹¹ gives 10.6 ± 0.2 eV. There is a further enhancement in the GeBr_4^+ signal at 1044 ± 8 Å (11.9 ± 0.1 eV). This is the same energy as the fourth peak in the photoelectron spectrum, which has been

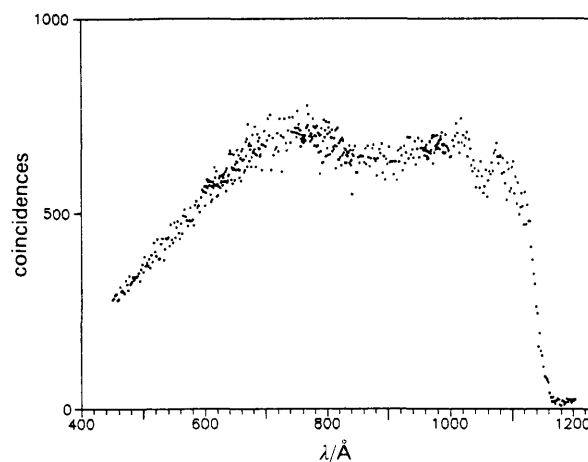


Fig. 8 Photoionisation yield of GeBr_4^+ from GeBr_4 in the range 450–1200 Å

assigned to the unresolved \tilde{A}^2T_2 (higher energy spin-orbit component) and \tilde{B}^2E states. As with SiBr_4 , neither total nor partial photoionisation cross-sections have been measured for GeBr_4 before. The ion-yield curve for GeBr_3^+ is shown in Fig. 9. The first threshold is observed at $1130 \pm 4 \text{ \AA}$ ($10.97 \pm 0.04 \text{ eV}$), and a steep increase in ion yield is observed at $1117 \pm 4 \text{ \AA}$ ($11.09 \pm 0.04 \text{ eV}$). This second threshold corresponds to the adiabatic E_i of the \tilde{A}^2T_2 first excited state of GeBr_4^+ . A third threshold is observed more weakly at $1048 \pm 8 \text{ \AA}$ ($11.82 \pm 0.09 \text{ eV}$), which is isoenergetic with $11.9 \pm 0.1 \text{ eV}$ for the vertical E_i of the $\tilde{A}^2T_2/\tilde{B}^2E$ states (see above). The broad peak at 770 \AA is almost certainly due to a shape resonance, and the apparent onset at *ca.* 880 \AA is unlikely to be a new threshold for GeBr_3^+ production.

The next ion channel to appear in ascending energy is GeBr^+ , and its ion-yield curve (after background subtraction) is shown in Fig. 10 for excitation wavelengths between 450 and 990 \AA . A threshold is observed at $910 \pm 10 \text{ \AA}$ ($13.6 \pm 0.1 \text{ eV}$). This energy lies within the Franck-Condon zone of the $\text{GeBr}_4^+ \tilde{C}^2T_2$ state which extends up to 14.1 eV .¹¹ However, the GeBr^+ threshold lies substantially higher in energy than the $\text{GeBr}_4^+ \tilde{C}^2T_2$ adiabatic E_i of $13.3_5 \pm 0.1 \text{ eV}$. It was noted in the introduction and elsewhere⁶ that the \tilde{C}^2T_2 state decays radiatively, and the threshold for fluorescence observed at $13.4 \pm 0.1 \text{ eV}$ confirmed this adiabatic E_i . The two spin-orbit components of \tilde{C}^2T_2 ($E_{5/2}$ and $G_{3/2}$) have vertical E_i s of 13.63 and 13.70 ,¹¹ although it is not clear which component corresponds to which E_i . It appears there-

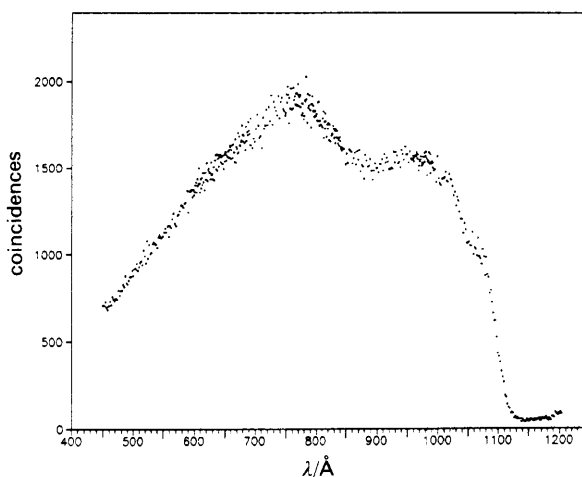


Fig. 9 Photoionisation yield of GeBr_3^+ from GeBr_4 in the range 450–1200 \AA

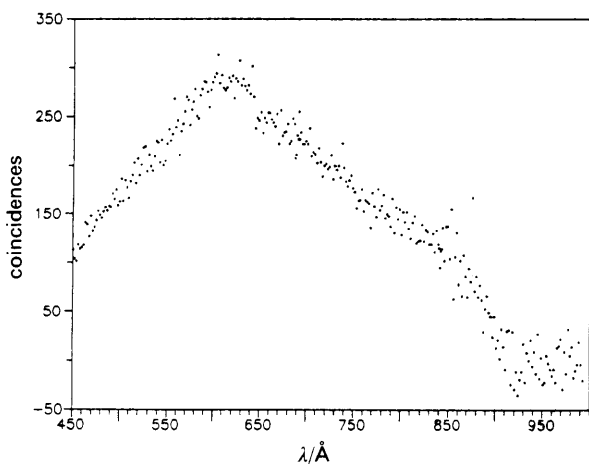


Fig. 10 Photoionisation yield of GeBr^+ from GeBr_4 in the range 450–990 \AA . False coincidences have been subtracted

fore that the GeBr^+ ion is produced by non-radiative decay from within the \tilde{C} -state manifold. We note that the lowest dissociation channel producing GeBr^+ has a thermochemical energy of 13.6 eV (Table 1).

No obvious increase is observed in any fragment channel around the energy of the \tilde{D}^2A_1 state of GeBr_4^+ at 17.6 eV . However, it is clear from the He I photoelectron spectrum that the branching ratio into \tilde{D}^2A_1 is very small ($<1\%$) at 21.2 eV ,¹¹ as is the case for the \tilde{D} state of similar molecules CF_4^+ ,¹⁶ SiF_4^+ ,¹⁷ CCl_4^+ ¹⁸ and SiCl_4^+ .¹⁹ If the \tilde{D} state of GeBr_4^+ dissociates into a fragment which is also produced by a lower electronic state with a greater cross-section (*e.g.* GeBr_3^+ or GeBr^+), the observation of a threshold at the \tilde{D} -state energy will be difficult. As commented elsewhere²⁰ this is a consequence of a lack of electron energy analysis in the present coincidence apparatus.

Above 21.2 eV the atomic ions Ge^+ and Br^+ appear. A He II photoelectron spectrum of GeBr_4 is not available and therefore a comparison of the thresholds with the energies of higher ionic states is not possible. There is also a major problem of mass resolution in that Ge has three major isotopes with mass 70, 72 and 74 (abundances 20, 27 and 36%, respectively) whilst Br exists as mass 79 and 81 with equal abundance. With the present experimental configuration these masses are sufficiently close to make complete mass resolution impossible. Thus in the 3D map⁹ the Ge^+/Br^+ peaks appear as a conglomerate, sloping from high TOF to low TOF as photon wavelength increases. A partial deconvolution has been possible, giving ion-yield curves for Ge^+ and Br^+ with thresholds of 580 ± 15 and $555 \pm 15 \text{ \AA}$, respectively.⁹ The normalised photoionisation mass-spectrometric branching ratios for GeBr_4 between 10.8 and 27.5 eV are shown in Fig. 11. All the observed thresholds for fragment ions from SiBr_4 and GeBr_4 are collected together in Table 2.

Kinetic Energy Releases

Virtually all of the ions studied in this work are affected by isotopic broadening. Br exists as ^{79}Br and ^{81}Br in equal abundance and therefore SiBr^+ will have two equally probable isotopic variants, whilst SiBr_4^+ will consist of five different combinations with statistical weights between one and six. With the extraction fields employed in the experiment, the differences in TOF peak positions corresponding to a mass difference of 2 u range from 65 ns for Br^+ to 31 ns for SiBr_4^+ . The situation is even less favourable for the GeBr_n^+ species because of the isotopic splitting in Ge (see above). All

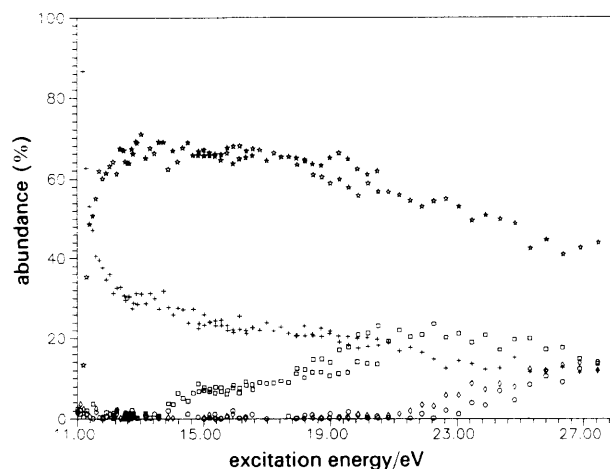


Fig. 11 Normalised photoionisation branching ratios for fragmentation of GeBr_4 between 11 and 27 eV . \diamond , Ge^+ ; \circ , Br^+ ; \square , GeBr_3^+ ; $+$, GeBr_4^+

Table 2 Observed thresholds^a for parent and fragment ions from vacuum UV photon excitation of SiBr₄ and GeBr₄

ion	threshold energy/eV	comment
SiBr ₄ ⁺	10.62 ± 0.04	SiBr ₄ ⁺ \tilde{X} adiabatic E_i
	11.38 ± 0.06	SiBr ₄ ⁺ \tilde{A} adiabatic E_i
	(12.25 ± 0.06)	
	(14.33 ± 0.08)	
SiBr ₃ ⁺	11.31 ± 0.03	SiBr ₃ ⁺ + Br thermochemical energy
	11.44 ± 0.03	SiBr ₄ ⁺ \tilde{A} adiabatic E_i
	(12.25 ± 0.06)	
SiBr ₂ ⁺	16.1 ± 0.3	
SiBr ⁺	17.1 ± 0.3	SiBr ₄ ⁺ \tilde{D} adiabatic E_i
Si ⁺	23.4 ± 0.4	
Br ⁺	25.0 ± 0.5	
GeBr ₄ ⁺	10.62 ± 0.04	GeBr ₄ ⁺ \tilde{X} adiabatic E_i
	(11.9 ± 0.1)	
GeBr ₃ ⁺	10.97 ± 0.04	GeBr ₃ ⁺ + Br thermochemical energy
	11.09 ± 0.04	GeBr ₄ ⁺ \tilde{A} adiabatic E_i
	(11.82 ± 0.09)	
	(14.1 ± 0.1)	
GeBr ⁺	13.6 ± 0.1	GeBr ⁺ + Br ₂ + Br thermochemical energy
Ge ⁺	21.4 ± 0.5	
Br ⁻	22.3 ± 0.6	

^a Values in parenthesis may not be due to genuine thresholds, but to enhancement in photoionisation cross-sections.

TOF spectra were recorded at 16 ns time resolution, no isotopic structure is resolved, and the data are not considered of sufficient quality to attempt a deconvolution procedure. The one ion not affected by isotopic broadening is Si⁺. The Si⁺ TOF peak has a half-width at half-maximum of 45 ± 8 ns, corresponding to an average KE release in the Si⁺ fragment of 0.17 ± 0.08 eV.⁸ This release is invariant to excitation energy above the Si⁺ threshold of 24.3 eV (see above).

Discussion

SiBr₄

The first threshold for production of SiBr₃⁺ + Br at 11.31 ± 0.03 eV lies in the high-energy portion of the \tilde{X} ²T₁ state photoelectron band of SiBr₄⁺, whilst the second much steeper threshold at 11.44 ± 0.03 eV corresponds to the adiabatic E_i of the lower spin-orbit component of the \tilde{A} ²T₂ state. Although these results do not reveal the fragmentation mechanism, dissociation of the \tilde{A} state is almost certainly direct and rapid from a repulsive potential surface. This would be similar to previous studies on the ground and first excited states of CF₄⁺^{7,21} and SF₆⁺^{8,22}. Vibrational levels of the ground state of SiBr₄⁺ below 11.31 eV are stable with respect to dissociation, whilst higher levels dissociate directly by loss of a bromine atom (see later). A conventional PEPICO experiment using the He I line as an excitation source and employing electron energy analysis could provide the detailed kinetic energy release distributions needed to establish the dissociation mechanism of these two states of SiBr₄⁺. A direct dissociation would explain the apparent continuous nature of both the SiBr₄⁺ \tilde{C} - \tilde{A} and \tilde{C} - \tilde{X} emission bands,⁶ if the Franck-Condon region of the \tilde{X} ²T₁ potential surface accessed by emission from the \tilde{C} state lies above the SiBr₃⁺ + Br dissociation limit. (Alternatively the continuous nature of the SiBr₄⁺ \tilde{C} - \tilde{X} band could just be due to a very large number of unresolved rovibrational components. There is some evidence that this is the case for the \tilde{C} - \tilde{X} band of SiCl₄⁺ centred at 410 nm.²³)

The threshold for SiBr₃⁺ + Br formation of 11.31 eV indi-

cates that there is a gross error in the literature value for the E_i of SiBr₃ of 12.5 ± 1.0 eV.¹³ When this E_i is combined with the heats of formation of SiBr₃ and SiBr₄ recommended by Walsh,¹² a thermochemical threshold for SiBr₃⁺ + Br of 16.2 eV is obtained (Table 1). This is 4.9 eV above the SiBr₃⁺ threshold observed in this work, and therefore suggests that the true E_i of SiBr₃ is 7.6 eV. However, two assumptions have been made. First, we assume that the experimentally observed threshold for SiBr₃⁺ production is identical to the thermodynamic dissociation energy of SiBr₃⁺ + Br. This is not true in the dissociation of CF₄⁺ \tilde{X} → CF₃⁺ + F because the CF₃⁺ + F thermodynamic energy is ca. 0.7 eV below the adiabatic E_i of the \tilde{X} state.⁷ However, with SiBr₄⁺ the SiBr₃⁺ + Br threshold lies within the Franck-Condon region of the \tilde{X} -state manifold, and the assumption will be true unless there is a substantial barrier to dissociation and/or a kinetic shift in the SiBr₃⁺ appearance energy.²⁴ Both are inconsistent with a direct dissociation mechanism. Secondly, the value used for the heat of formation of SiBr₃ is assumed to be known accurately. In fact this may not be so, and Walsh did not place great confidence in his recommended value of -1.65 ± 0.26 eV.¹² Farber and Srivastava¹³ obtained -2.05 ± 0.12 eV whilst the latest JANAF tables²⁵ quote -2.1 ± 0.6 eV. We use the maximum difference between these values (ca. 0.4 eV) as a generous estimate of the error, and therefore quote the E_i of SiBr₃ as 7.6 ± 0.4 eV.

It now appears that there is a systematic error in the ionisation potentials of SiBr_n as measured by Farber and Srivastava.¹³ In addition to the SiBr₃ E_i which is 4.9 eV too high, these authors also measured the E_i s of SiBr and SiBr₄ to be 9 ± 1 and 14 ± 1 eV, respectively. These values are 2.3 and 3.4 eV above the accurate E_i s measured by Rydberg spectroscopy²⁶ and this work, respectively. We therefore suggest that the E_i of SiBr₂ as measured by Farber and Srivastava be lowered by 3.5 eV (the mean of the other errors), giving 8.5 ± 1.5 eV. Unfortunately there is no other direct measurement (e.g. by photoelectron spectroscopy) of the E_i of SiBr₂.

This revised E_i for SiBr₂ places the thermochemical energies of the SiBr₂⁺ + Br₂ and SiBr₂⁺ + Br + Br channels at 12.3 and 14.3 eV, respectively. Thus channels into both SiBr₂⁺ and SiBr⁺ are energetically available to the \tilde{C} ²T₂ state of SiBr₄⁺ (Table 1), yet these ions have appearance thresholds at much higher energies. We have shown⁶ that the \tilde{C} state decays radiatively with a long lifetime (47.6 ns) which is invariant to excitation energy. This strongly suggests that the fluorescence quantum yield of this state is unity and that no non-radiative process competes with fluorescence. The observed threshold for production of SiBr₂⁺ is 16.1 ± 0.3 eV, and channels to both Br₂ and Br + Br as the other product are energetically open. The source of this SiBr₂⁺ signal is not clear. It is not due to second-order radiation, it does not appear to originate from an electronic state of SiBr₄⁺ and its threshold is in the Franck-Condon gap, i.e. in the energy region between the Franck-Condon zones of parent ion electronic states accessed by direct photoionisation. It may be produced by autoionisation of a neutral Rydberg state into highly excited levels of a lower electronic state which display different dissociation dynamics to the states populated by direct photoionisation. However, this explanation can only be regarded as tentative, not least because there is no spectroscopic information available on Rydberg states of SiBr₄ in the extreme vacuum UV.

The threshold for SiBr⁺ formation of 17.1 ± 0.3 eV lies 3.1 eV above the lowest thermochemical channel involving SiBr⁺ (Table 1). This threshold is equivalent to the adiabatic E_i of the \tilde{D} ²A₁ state of SiBr₄⁺. From our previous fluorescence studies⁶ it is known that this state decays non-radiatively, and we therefore suggest that this state fragments to SiBr⁺.

The nature of the other products (3Br or $\text{Br} + \text{Br}_2$) cannot be determined. We note that the $\tilde{\text{D}}^2\text{A}_1$ states of CCl_4^+ , SiCl_4^+ and GeCl_4^+ all decay non-radiatively by fragmentation to CCl_2^+ , SiCl_2^+ and GeCl_2^+ and GeCl_2^+ , respectively.⁷ The $\tilde{\text{D}}$ states of the three fluorides all decay radiatively,⁵ probably with a fluorescence quantum yield of unity.

The Si^+ and Br^+ thresholds at 23.4 and 25.0 eV, respectively, lie many eV above the lowest available dissociation channels. Thus the Si^+ threshold is 7.1 eV above the $\text{Si}^+ + \text{Br}_2 + \text{Br}_2$ channel, and the Br^+ threshold is 9.5 eV above the channel to $\text{SiBr}_3 + \text{Br}^+$ (Table 1). It seems likely that both the Si^+ and Br^+ ions are associated with the complete fragmentation of the parent ion, *i.e.* the $\text{Si}^+ + 4\text{Br}$ channel at 20.3 eV and the $\text{Si} + 3\text{Br} + \text{Br}^+$ channel at 22.9 eV are operative. This would be consistent with the relatively low kinetic energy release into the Si^+ ion of 0.17 ± 0.08 eV. Our results cannot provide an answer as to whether the dissociations are simultaneous or stepwise.

GeBr₄

The GeBr_3^+ fragment appears initially at an energy of 10.97 ± 0.04 eV. Thus, as with SiBr_4^+ , the threshold for GeBr_3^+ production lies within the $\text{GeBr}_4^+ \tilde{\text{X}}$ state manifold, and very similar comments to those made above concerning $\text{SiBr}_4^+/\text{SiBr}_3^+ + \text{Br}$ apply here. A value for the E_i of GeBr_3^+ is not available in the literature, but an electron-impact appearance energy of GeBr_3^+ from GeBr_4 is known.¹⁴ This value of 11.0 ± 0.3 eV compares excellently with the more accurate photoionisation threshold reported here. The heat of formation for GeBr_3 has not been measured, and therefore the E_i of GeBr_3 cannot be calculated.

Our previous work⁶ showed that the $\tilde{\text{C}}^2\text{T}_2$ state of GeBr_4^+ decayed radiatively *via* $\tilde{\text{C}}-\tilde{\text{A}}$ and $\tilde{\text{C}}-\tilde{\text{X}}$ emissions with a lifetime of 67 ns. The threshold for fluorescence, 13.4 ± 0.1 eV,⁶ agreed excellently with the adiabatic E_i of the lower spin-orbit component of $\tilde{\text{C}}$ of 13.35 ± 0.08 eV.¹¹ This PIMS study has shown that the GeBr^+ fragment has a threshold of 13.6 ± 0.1 eV within the Franck-Condon zone of the $\tilde{\text{C}}$ state. The lowest thermochemical channel involving GeBr^+ is at 13.6 eV with the next channel (to $\text{GeBr}^+ + \text{Br} + \text{Br} + \text{Br}$) at 15.6 eV. Therefore the production of GeBr^+ must be accompanied with the $\text{Br}_2 + \text{Br}$ products, and it is likely that the fragmentation threshold is at the thermodynamic limit for this process. It would be interesting to know the rate at which non-radiative fragmentation to GeBr^+ occurs. If dissociation is sufficiently rapid ($\geq 1 \times 10^{10} \text{ s}^{-1}$) the fluorescence quantum yield of $\tilde{\text{C}}$ vibrational levels above the GeBr^+ threshold will drop to undetectable levels ($\leq 10^{-3}$), and the 67 ns lifetime would relate only to those levels below the GeBr^+ dissociation limit. At the other extreme, a very slow ($\leq 10^8 \text{ s}^{-1}$) dissociation would result in a sizeable quantum yield ($\Phi_{\text{hv}} \geq 0.1$) for levels above the GeBr^+ threshold and a reduced lifetime. In such a scenario a reduction in measured lifetime with increasing excitation energy above the GeBr^+ threshold may be apparent as the contribution from predissociating levels becomes more important. This effect was seen for the $\tilde{\text{C}}^2\text{T}_2$ state of CF_4^+ where radiative decay competes with slow fragmentation to CF_2^+ , and the measured lifetime dropped from 9.66 ns to 8.58 ns at 2 eV above the $\tilde{\text{C}}$ state threshold.⁵ However with the $\tilde{\text{C}}$ state of GeBr_4^+ , the lifetime was measured at only one excitation energy (22.5 eV) well above threshold,⁶ because the fluorescence signal nearer threshold was low. In any case, this method of observing changes in lifetime is not very satisfactory because the measured lifetime is a convolution of decays from all levels populated by photoionisation. A threshold photoelectron-

fluorescence photon coincidence experiment should provide useful information. This technique measures fluorescence lifetimes and quantum yields as a function of parent-ion internal energy, and hence could reveal (a) if levels of the $\text{GeBr}_4^+ \tilde{\text{C}}$ state above the GeBr^+ threshold fluoresce with sizeable quantum yield, and (b) what the lifetimes of fluorescing levels above and below the GeBr^+ threshold are. The mechanism for fragmentation into GeBr^+ is unknown. It could involve a simultaneous or sequential dissociation, the latter process involving either the GeBr_2^+ or GeBr_3^+ intermediates.

Our fluorescence study⁶ showed that the $\tilde{\text{D}}^2\text{A}_1$ state of GeBr_4^+ does not decay radiatively, and it is therefore disappointing that there is no apparent increase in the signal of any ionic fragment at the $\tilde{\text{D}}$ state energy. However, the photoionisation branching ratio of this state is expected to be very small, and the lack of any electron energy analyser in our experiment means that it will be difficult to observe an increase in a fragment signal (say GeBr_3^+) on top of a large signal already present from fragmentation of lower states. The Ge^+ and Br^+ ions appear *ca.* 7 eV above the lowest available dissociation limits, a situation very similar to the formation of Si^+ and Br^+ from SiBr_4 . As with these latter ions, it is suggested that Ge^+ and Br^+ result from complete fragmentation of GeBr_4 to $\text{Ge}^+ + 4\text{Br}$ and $\text{Ge} + 3\text{Br} + \text{Br}^+$, respectively. The experimentally observed Br^+ threshold of 22.8 ± 0.7 eV occurs within error limits at the threshold energy of this latter channel of 22.4 eV.

The tetrabromo molecular ions SiBr_4^+ and GeBr_4^+ show similar, but not identical, non-radiative decay properties to their tetrachloro counterparts.⁷ Their ground and first two excited states ($\tilde{\text{X}}$, $\tilde{\text{A}}$ and $\tilde{\text{B}}$) behave identically. The dissociation channel to $\text{MX}_3^+ + \text{X}$ lies within the Franck-Condon region of the ground state of MX_4^+ , thus low vibrational levels show the properties of a bound state whereas higher levels above the dissociation channel are dissociative. The $\tilde{\text{A}}$ and $\tilde{\text{B}}$ states of these ions are probably totally repulsive states in all parts of the multi-dimensional potential. The $\tilde{\text{C}}$ states are bound and decay radiatively by the relatively slow process of photon emission ($k \approx 10^7\text{--}10^8 \text{ s}^{-1}$). Although we have not shown this directly, it is suspected that the fluorescence quantum yield of these $\tilde{\text{C}}$ states is unity (for SiCl_4^+ , GeCl_4^+ , SiBr_4^+) or close to unity (for GeBr_4^+). Radiative decay is very surprising in this instance because several dissociation channels are energetically open, and in a five-atom polyatomic non-radiative processes would be expected to occur much more rapidly than photon emission. The $\tilde{\text{D}}$ states of MX_4^+ all decay non-radiatively, but to different products. Thus the $\tilde{\text{D}}$ state of SiCl_4^+ dissociates to SiCl_2^+ ,⁷ GeCl_4^+ to both GeCl_2^+ and GeCl^+ ,⁷ and SiBr_4^+ to SiBr^+ . The dissociation products of $\text{GeBr}_4^+ \tilde{\text{D}}$ could not be determined in this study. CBr_4 was not studied in our experiment due to its low vapour pressure. CCl_4 behaves differently from SiCl_4 and GeCl_4 in the behaviour of its $\tilde{\text{C}}$ ionic state; it dissociates on a rapid timescale ($> 10^{10} \text{ s}^{-1}$) to CCl_2^+ which means that fluorescence cannot compete.⁷ It is likely that fragmentation of the ionic states of CBr_4 mimics those of CCl_4 .

In SiBr_4^+ and GeBr_4^+ the appearance energies of fragment ions can be correlated with electronic states of the parent ion, not to the lowest thermochemical threshold for that ion, and they therefore appear above the thermochemical or thermodynamic energy. (The exceptions are SiBr_3^+ and GeBr_3^+ which turn on initially at the SiBr_3^+ (GeBr_3^+) + Br thermodynamic energy, since they lie in the Franck-Condon region of the parent-ion ground state. GeBr^+ may also initially turn on at the $\text{GeBr}^+ + \text{Br}_2 + \text{Br}$ thermodynamic energy.) Similar behaviour has been observed previously for the Group 14 tetrafluoro and tetrachloro molecular ions⁷ and for SF_6^+ ,⁸ but is not general for polyatomic ions.^{27,28} The conventional

view of polyatomic ion dissociation is that the initial ionisation process (in this case by photoionisation) serves only to create the polyatomic ion in a range of electronic states. Equilibration then takes place so rapidly (*e.g.* by internal conversion) that one only considers the density of vibrational levels of the ground electronic state in determining the fragmentation pattern. These levels dissociate by all energetically available pathways at rates which are usually well predicted by statistical theories²⁹ (*e.g.* quasi-equilibrium theory).³⁰ However this picture of polyatomic ion dissociation depends on the existence of a strongly bound ground state to which the application of statistical methods is valid. The ground states of CF_4^+ ⁷ and SF_6^+ ⁸ are totally repulsive, and therefore theories which invoke vibrational energy randomisation are inappropriate for these ions. The situation is not so clear for SiBr_4^+ and GeBr_4^+ because the ground states of these ions are partially bound with well depths of *ca.* 0.7 and 0.5 eV, respectively. However the dissociation dynamics of other electronic states of these ions behave similarly to CF_4^+ and SF_6^+ , and therefore it appears that above the $\text{MBr}_3^+ + \text{Br}$ dissociation energy the ground states of SiBr_4^+ and GeBr_4^+ are essentially repulsive in nature. Two further points are worth noting. First, although there may be one example (SiBr_2^+) of an ion appearing in the Franck–Condon gap following photoexcitation of SiBr_4 and GeBr_4 , the observed threshold is still *ca.* 4.4 eV above the new value for the thermodynamic threshold. Secondly, the relatively slow process of radiative decay (on the ns or slower timescale) is not considered a fast enough de-activation route for excited electronic states of a polyatomic ion to form the ground state for subsequent statistical fragmentation. In other words, radiative decay from excited states lying above several dissociation channels can be thought of as one manifestation of a non-statistical process.

Conclusion

Future experiments have largely been suggested in previous sections of the paper. They include coincidence experiments involving some kind of electron energy analysis (He I photoelectron–photoion, threshold photoelectron–photoion, and threshold photoelectron–fluorescence) which could provide further information on dissociation mechanisms. High-resolution spectroscopic information is lacking because of the absence of discrete structure in the SiBr_4^+ and GeBr_4^+ $\tilde{\text{C}}-\tilde{\text{A}}$ and $\tilde{\text{C}}-\tilde{\text{X}}$ emission bands. However, the ground states of these two ions are partially bound, resulting in sizeable parent-ion signals in the TOF mass spectra. It may be possible to apply laser-induced fluorescence techniques to the $\tilde{\text{C}} \leftarrow \tilde{\text{X}}$ transition. These states have symmetry $^2\text{T}_2$ and $^2\text{T}_1$, respectively, and will exhibit a number of interesting spectroscopic effects such as spin–orbit splitting³¹ and Jahn–Teller distortion. The dissociation mechanisms of the valence electronic states of SiBr_4^+ and GeBr_4^+ to fragment ions are largely unknown, but they will depend on the exact positions and crossing points of other repulsive potential curves of doublet and quartet spin symmetry. *Ab initio* calculations have been reported on the five valence doublet electronic states of CF_4^+ , SiF_4^+ and GeF_4^+ ,³² but there have been no calculations yet on the doublet and quartet states of the heavier chloride and bromide ions. Such calculations are needed to understand in further detail the dissociation mechanisms of the valence states of MBr_4^+ .

In summary, we have presented a photoionisation mass spectrometry study of SiBr_4 and GeBr_4 between 400 and 1220 Å over the range of the five lowest valence states of the parent ion. Ion-yield curves have been obtained for both the parent ion and the fragment ions formed in this photon

range, as well as the relative photoionisation branching ratios. We have obtained a new value for the ionisation potential of SiBr_3 , and we suggest that the previously accepted value for SiBr_2 is *ca.* 3.5 eV too high.

We thank the staff at the Daresbury Laboratory (especially Drs. D. M. P. Holland, A. Hopkirk, M. Hayes and J. B. West) for assistance, and Dr. J. F. M. Aarts for helpful discussions. We also thank the SERC for Research Studentships (J.C.C., I.R.L.), a Research Fellowship (P.A.H.), a Visiting Fellowship (M.S.) and an equipment grant.

References

- 1 J. F. M. Aarts, S. M. Mason and R. P. Tuckett, *Mol. Phys.*, 1987, **60**, 761.
- 2 S. M. Mason and R. P. Tuckett, *Mol. Phys.*, 1987, **60**, 771.
- 3 S. M. Mason and R. P. Tuckett, *Mol. Phys.*, 1987, **62**, 979.
- 4 I. R. Lambert, S. M. Mason, R. P. Tuckett and A. Hopkirk, *J. Chem. Phys.*, 1988, **89**, 2675.
- 5 I. R. Lambert, S. M. Mason, R. P. Tuckett and A. Hopkirk, *J. Chem. Phys.*, 1988, **89**, 2683.
- 6 J. C. Creasey, I. R. Lambert, R. P. Tuckett and A. Hopkirk, *J. Chem. Soc., Faraday Trans.*, 1990, **86**, 2021.
- 7 J. C. Creasey, I. R. Lambert, R. P. Tuckett, K. Codling, L. J. Frasinski, P. A. Hatherly, M. Stankiewicz and D. M. P. Holland, *J. Chem. Phys.*, 1990, **93**, 3295.
- 8 J. C. Creasey, I. R. Lambert, R. P. Tuckett, K. Codling, L. J. Frasinski, P. A. Hatherly and M. Stankiewicz, *J. Chem. Soc., Faraday Trans.*, 1991, **87**, 1287.
- 9 I. R. Lambert, Ph.D. Thesis, University of Birmingham, 1991.
- 10 W. C. Wiley and I. H. McLaren, *Rev. Sci. Instrum.*, 1955, **26**, 1150.
- 11 J. C. Green, M. L. H. Green, P. J. Joachim, A. F. Orchard and D. W. Turner, *Philos. Trans. R. Soc. London, Ser. A*, 1970, **268**, 111.
- 12 R. Walsh, *J. Chem. Soc., Faraday Trans. 1*, 1983, **79**, 2233.
- 13 M. Farber and R. D. Srivastava, *High Temp. Sci.*, 1980, **12**, 21.
- 14 O. Uy Manual, D. W. Muenow and J. L. Margrave, *Trans. Faraday Soc.*, 1969, **65**, 1296.
- 15 J. Berkowitz, *Photoabsorption, Photoionisation and Photoelectron Spectroscopy*, Academic Press, New York, 1979.
- 16 T. A. Carlson, A. Fahlman, W. A. Svensson, M. O. Krause, T. A. Whitley, F. A. Grimm, M. N. Piancastelli and J. W. Taylor, *J. Chem. Phys.*, 1984, **81**, 3828.
- 17 B. W. Yates, K. H. Tan, G. M. Bancroft, L. L. Coatsworth and J. S. Tse, *J. Chem. Phys.*, 1985, **83**, 4906.
- 18 T. A. Carlson, M. O. Krause, F. A. Grimm, P. Keller and J. W. Taylor, *J. Chem. Phys.*, 1982, **77**, 5340.
- 19 T. A. Carlson, A. Fahlman, M. O. Krause, T. A. Whitley, F. A. Grimm, M. W. Piancastelli and J. W. Taylor, *J. Chem. Phys.*, 1986, **84**, 641.
- 20 R. P. Tuckett, *Chem. Soc. Rev.*, 1990, **19**, 439.
- 21 I. Powis, *Mol. Phys.*, 1980, **39**, 311.
- 22 I. G. Simm, C. J. Danby, J. H. D. Eland and P. I. Mansell, *J. Chem. Soc., Faraday Trans. 2*, 1976, **72**, 426.
- 23 J. F. M. Aarts, unpublished results.
- 24 T. Baer, *Comm. At. Mol. Phys.*, 1983, **13**, 141.
- 25 M. W. Chase, C. A. Davies, J. R. Downey, D. J. Frurip, R. A. McDonald and A. N. Syverud, *J. Phys. Chem. Ref. Data*, 1985, **14**, suppl. 1.
- 26 G. Bossert, H. Bredohl and I. Dubois, *J. Mol. Spectrosc.*, 1984, **106**, 72.
- 27 O. Dutuit, M. Ait-Kaci, J. Lemaire and M. Richard-Viard, *Phys. Scr.*, 1990, **T31**, 223.
- 28 T. Baer, P. M. Guyon, I. Nenner, A. Tabache-Fouhaille, R. Botter, L. F. A. Ferreira and T. R. Govers, *J. Chem. Phys.*, 1979, **70**, 1585.
- 29 T. Baer, in *Adv. Chem. Phys.*, ed. I. Prigogine and S. A. Rice, John Wiley and Sons, New York, 1986, vol. LXIV.
- 30 H. M. Rosenstock, *Adv. Mass Spectrom.*, 1968, **4**, 523.
- 31 R. N. Dixon and R. P. Tuckett, *Chem. Phys. Lett.*, 1987, **140**, 553.
- 32 R. A. Bearda, H. R. R. Wiersinga, J. F. M. Aarts and J. J. C. Mulder, *Chem. Phys.*, 1989, **137**, 157.